

Relative contributions of the weak, main and fission-recycling r -process

S. Shibagaki^{1,2}, T.Kajino^{1,2}, G. J. Mathews^{1,3}, S. Chiba⁴, S. Nishimura^{1,5}, and G. Lorusso⁵

¹ *Division of Theoretical Astronomy, NAOJ, 181-8588 Mitaka, Japan*

² *Department of Astronomy, The University of Tokyo, 113-033 Tokyo, Japan*

³ *Center for Astrophysics, Department of Physics,
University of Notre Dame, Notre Dame, IN 46556, USA*

⁴ *Research Laboratory for Nuclear Reactors, Tokyo Institute of Technology,
2-12-1 Ookayama, Meguro, Tokyo 152-8550, Japan and*

⁵ *RIKEN Nishina Center, 2-1 Hirosawa, Wako-shi, Saitama 351-0198, Japan*

(Dated: March 27, 2019)

There has been a persistent conundrum in attempts to model the nucleosynthesis of heavy elements by rapid neutron capture (the r -process). Although the location of the abundance peaks near nuclear mass numbers 130 and 195 identify an environment of rapid neutron capture near closed nuclear shells, the abundances of elements just above and below those peaks are often underproduced by more than an order of magnitude in model calculations. At the same time there is a debate in the literature as to what degree the r -process elements are produced in supernovae or the mergers of binary neutron stars. In this paper we propose a novel solution to both problems. We demonstrate that the underproduction of elements above and below the r -process peaks characteristic in the main or weak r -process events (like magnetohydrodynamic jets or neutrino-driven winds in core-collapse supernovae) can be supplemented via fission fragment distributions from the recycling of material in a neutron-rich environment such as that encountered in neutron star mergers. In this paradigm, the abundance peaks themselves are well reproduced by a moderately neutron rich, main r -process environment such as that encountered in the magnetohydrodynamical jets in supernovae supplemented with a high-entropy, weakly neutron rich environment such as that encountered in the neutrino-driven-wind model to produce the lighter r -process isotopes. Moreover, we show that the relative contributions to the r -process abundances in both the solar-system and metal-poor stars from the weak, main, and fission-recycling environments required by this proposal are consistent with estimates of the relative Galactic event rates of core-collapse supernovae for the weak and main r -process and neutron star mergers for the fission-recycling r -process.

PACS numbers: 24.75.+i, 25.85.-w, 26.30.Hj, 26.50.+x, 97.60.Bw

I. INTRODUCTION

It has been known for more than half a century [1] that about half of the elements heavier than iron are produced via rapid neutron capture (the r -process). Indeed, the basic physical conditions for the r -process are well constrained [1] by simple nuclear physics. The observed abundance distribution requires a sequence of near equilibrium rapid neutron captures and photoneutron emission reactions far on the neutron-rich side of stability. This equilibrium is established with a maximum abundance strongly peaked on one or two isotopes far from stability. The relative abundance of r -process elements is then determined by the relative β -decay rates along this r -process path., i.e., longer β -decay lifetimes result in higher abundances.

In spite of this simplicity, however, the unambiguous identification of the site for the r -process nucleosynthesis has remained elusive. Parametrically, one can divide current models for the r -process into three scenarios roughly characterized by the number of neutron captures per seed nucleus (n/s). This parameter, in turn is the consequence of a variety of conditions such as time-scale, baryon density, average charge per baryon, $Y_e \equiv \langle Z/A \rangle$, and entropy (or baryon to photon ratio) corresponding to different astrophysical environments (e.g. [2, 3]). An environment in

which there are few neutron captures per seed ($n/s \sim 50$) produces what has been identified as the weak r -process [4] and can only produce the lightest r -process nuclei up to $A \sim 125$. Such an environment could occur, for example, in the neutrino-driven wind of core-collapse supernovae (CCSNe) [5, 6]. An environment with enough neutron captures per seed ($n/s \sim 100$) to produce the two r -process abundance peaks at $A = 130$ and 195, corresponds to what has been dubbed the main r -process and could correspond, for example, to the ejection of neutron-rich material via magnetic turbulence in magnetohydrodynamically driven jets (MHDJ) from core collapse supernovae ([7–12]. In this paper, we also are interested in a third environment which we dub the fission-recycling r -process. In this environment the number of neutron captures per seed nucleus can be very large ($n/s \sim 1000$). The r -process path then proceeds along the neutron drip line all the way to the region of fissile nuclei ($A \approx 300$) in which the r -process is terminated by beta- or neutron-induced fission. Fission recycling then occurs whereby after fissioning, the fission fragments continue to experience neutron captures until beta- or neutron-induced fission again terminates the r -process path. After a few cycles the abundances can become dominated by the fission fragment distributions and not as much by the beta-decay flow near the closed shells. Hence, a very differ-

ent mass distribution can ensue. Such environments are often associated with neutron star mergers (NSMs) in which the tidal ejection of neutron-rich material during the merger can lead to fission recycling and many neutron captures per seed (e.g. [13–17]).

Observations [18] showing the appearance of heavy-element r -process abundances early in the history of the Galaxy seem to favor the short progenitor lifetime of CC-SNe over NSMs as the r -process site. However, identifying the r -process site in models of CCSNe has been difficult [19, 20].

The three types of environments, neutrino-driven winds (NDWs), magnetohydrodynamic jets (MHDJs), and neutron star mergers (NSMs), have all been studied extensively in the recent literature. The robustness of the results varies for different environments, but uncertainties in both astrophysical conditions and nuclear input are well recognized in all cases. For example, the previously popular model [5] of r -process nucleosynthesis in the NDW above the newly forming neutron star has recently been shown [21, 22] to be inadequate as a main r -process site when modern neutrino transport methods have been employed. The required neutron captures per seed does not occur in the neutrino energized wind. Nevertheless, it is quite likely that the weak r -process does occur [6] in the NDW producing neutron rich nuclei up to about $A \sim 125$.

Indeed, the difficulties in reproducing the r -process abundances have motivated many new studies of NSMs (e.g. [13–15, 23, 24]). Nevertheless, one scenario for the r -process in CCSNe remains viable. It is the magnetohydrodynamic supernova jet (MHDJ) model [7–12]. In this model magnetic turbulence leads to the ejection of neutron rich material into a jet. As the jet transports this neutron-rich material away from the star it can undergo r -process nucleosynthesis in a way that avoids the low neutron-to-seed ratio associated with neutrino interactions in the NDW model. Moreover, the required conditions of the r -process environment (timescale, neutron density, temperature, entropy, electron fraction, etc.) are well accommodated in this model.

However, there is a persistent problem in this model, or any general model (e.g. [2, 3]) in which the r -process elements are produced in a short time scale via the rapid expansion of material away from a neutron star. In such models, the neutron density rapidly diminishes and r -process path freezes out near the neutron closed shells far from stability. Most such models underproduce isotopic abundances just below and above the r -process abundance peaks as we describe in more detail below.

With this in mind our goal in this study is to analyze the general advantages and disadvantages of each of the characteristic environments. Although we have noted here specific astrophysical models that are likely to be associated with the various conditions, the readers should be aware of the uncertainties involved and consider these environments as illustrative, not definitive. Nevertheless, we seek here to quantify the relative contribution

of each scenario to the observed solar-system r -process abundance distribution and the distribution of r -process elements in the early Galaxy. The novel conclusion of this paper is that one can utilize the inherent shortcomings of the three characteristic environments to *quantify* for the first time the relative contributions of each possible environment (weak, main, and fission recycling) to the final observed r -process abundances.

II. EFFECT OF NUCLEAR CLOSED SHELLS

Figure 1 illustrates why the abundances below and above the r -process peaks are bypassed. It shows an example of a typical calculated r -process path near the $N = 82$ neutron closed shell just before freezeout when the neutrons are rapidly exhausted and the abundances begin to beta decay back to the region of stable isotopes. Neutron captures and photo-neutron emission proceed in equilibrium for nuclei with a neutron binding energy of about 1-2 MeV. Above and below a closed neutron shell, however, this r -process path shifts abruptly toward the closed shell from below (or away from the closed shell for higher nuclear masses). This shifting of the r -process path toward the $N = 82$ neutron closed shell causes isotopes with $N = 70 - 80$ ($A \sim 110-120$) to be bypassed. Similarly, the $A = 140-147$ underproduction corresponds to the isotopes with proton closed shell $Z = 50$ and $N \sim 90-97$ ($A \sim 140-147$). These isotopes will also be bypassed in the beta-decay flow as is evident on Figure 1.

We emphasize that this is not just an artifact of the particular mass model employed in this study. All of the models in the current literature with a rapid freezeout (including the MHDJ[7–12]) show this underproduction if the final abundances are normalized to the abundance peaks. Indeed, one is hard pressed to find any model for the main r -process (including NDW models) in which this underproduction does not occur.

One can of course contrive calculations to somewhat fill the dips on both sides of the second r -abundance peak (for example, calculations using the ETFSI mass model as displayed in Fig. 7 in Ref. [7]). However, these models do so at the cost of displacing the 2nd and 3rd peaks and/or underproducing (or overproducing) abundances over a wide mass region between the second and third peaks. This was also a consistent feature in the original realistic NDW models of Ref. [5]. Indeed this effect is apparent in almost every r -process calculation since the 1970s (cf. review in Ref. [25]).

Although it has been speculated for some time (e.g. Ref. [5, 26, 27]) that this could be due to quenching of the strength of the shell closure or beta-decay rates near the closed neutron shell, this explanation is unlikely. Recent r -process calculations [28] based upon new measurements [29] of beta-decay half lives near the $A = 130$ r -process path have confirmed the absence of shell quenching effects in the beta flow. Moreover, recently the first

ever studies [30] of the level structure of the waiting-point nucleus ^{128}Pd ($Z=46$, $N=82$ in Fig. 1) and ^{126}Pd have been completed. This study clearly indicates that the shell closure at the neutron number $N=82$ is fairly robust. Hence, there is absolutely no evidence of the hypothesized quenching effects in either the beta decay rates of nuclear masses. One must suppose that some other resolution of this underproduction is necessary.

One goal of this paper is, therefore, to point out that a solution to the underproduction of nuclei above and below the r -process abundance peaks can be obtained if one considers that a fission recycling environment (e.g. NSMs) has contributed to the solar-system r -process abundance distribution in addition to the environments responsible for the weak and main r -process (like CC-SNe). Indeed, this novel solution not only resolves this dilemma but can *quantify* the answer to the question of the relative contributions to the r -process abundances of the weak and main r -process environments (such as those due to CCSNe) vs. long-duration fission-recycling environments (such as NSMs).

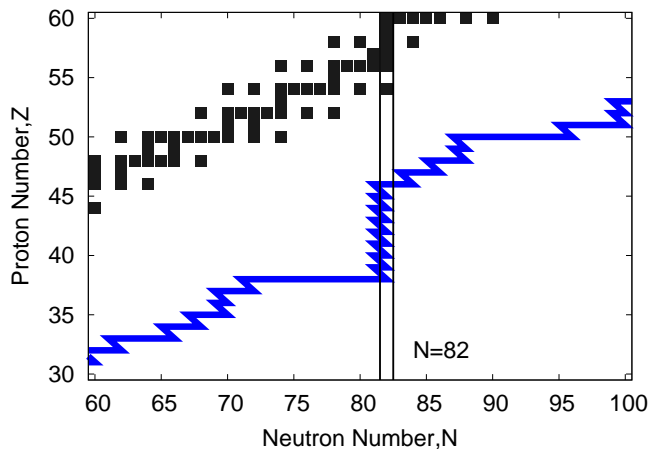


FIG. 1: (Color online) Illustration of the (N,Z) path of r -process nucleosynthesis (blue line) for nuclei with $A \sim 90 - 150$ in the vicinity of the $N = 82$ neutron closed shell and $Z=50$ proton closed shell just before freezeout of the abundances in a typical main r -process (MHDJ) model. Black squares show the stable isotopes.

III. FISSION RECYCLING r -PROCESS

For this paper we highlight the possible role of fission recycling to account for the underproduction problem above and below the r -process peaks often found in models for the main r -process abundances. For our purposes we employ a specific NSM model although we note that this is illustrative of any fission-recycling r -process environment. Nevertheless, the most natural current site

for such fission recycling to occur is in the NSM models. The ejected matter from NSMs is very neutron-rich ($Y_e \sim 0.1$). This means that the r -process path proceeds along the neutron drip line all the way to the onset of fission recycling. As noted above, after a few cycles the abundances can become dominated by the fission fragment distributions and not as much by the beta-decay flow near the closed shells. Hence, a very different mass distribution can ensue.

In this regard we note that a number of recent studies [13–15, 23, 24] have indicated that the r -process in NSMs can involve a distribution of neutron-rich environments. Such models can produce a final abundance pattern that is similar to the solar-system r -abundances. Here, even though we use the term NSM model, it is intended to refer to the portion of the ejecta that experiences fission recycling, while the other ejecta is similar to a NDW or MHDJ like model. Hence, when we refer to the NSM model we really mean the ejecta that experiences fission recycling that fills in the bypassed abundances produced in trajectories that produce the main r -process.

An important point is that models including fission recycling effects produce a final abundance pattern that is relatively insensitive to the astrophysical uncertainties [14], although the total (including non-recycling ejecta) abundances can be sensitive to the detailed model.

Nevertheless, the distribution of nuclear fission products can affect the abundance pattern. Hence, one must carefully extrapolate fission fragment distributions (FFDs) to the vicinity of the r -process path (cf. [31, 32]). We argue that by incorporating the expected broad distribution of fission fragments based upon phenomenological fits to observed FFDs, the effect of the neutron closed shells becomes smoothed out, thereby providing a means to fill in the isotopes bypassed in the main r -process.

For the present study we have made use of self consistent β -decay rates, β -delayed neutron emission probabilities, and β -delayed fission probabilities taken from Chiba et al. [33]. The spontaneous fission rates and the α -decay rates are taken from [34]. In our r -process calculations, β -delayed fission is the dominant nuclear fission mode. Hence, for the most part other fission modes like neutron-induced fission are unimportant [33].

To generate FFDs far from stability we have made use of a semi-empirical model [33, 35, 36] that well reproduces the systematics of known fission fragment distributions. In particular it is necessary to account for FFDs that can either be single humped, bimodal or even trimodal. In the model invoked here, this is achieved by a weighted superposition of up to three Gaussian functions:

$$f(A, A_p) = \sum_{A_i} \frac{1}{\sqrt{2\pi}\sigma} W_i \exp\left(\frac{-(A - A_i)^2}{2\sigma^2}\right), \quad (1)$$

where A is the mass number of each fission fragment, A_p is that of the parent nucleus, σ is the width of the three Gaussian functions, and the sum is over the possible

fission fragment distributions, $i = L, H, M$, with

$$A_H = \frac{(1 + \alpha)}{2}(A_p - N_{loss}) , \quad (2)$$

$$A_L = \frac{(1 - \alpha)}{2}(A_p - N_{loss}) , \quad (3)$$

and

$$A_M = \frac{(A_H + A_L)}{2} . \quad (4)$$

The factor W_i is a weighting given by $(1 - \omega_s)$ for $i = L, H$ and $2\omega_s$ for $i = M$. The quantities ω_s and α are shape symmetry and mass-asymmetry parameters, respectively as defined below. N_{loss} is the number of prompt neutrons.

For the present application we include the dispersion in the FFDs ($\sigma = 7.0$) and $N_{loss} = 2$ from measured experiments on actinides. The adopted fission neutron emission is an average value for all possible fission events. We have run calculations in which this number N_{loss} is varied from 2 to 8 and found that the results are nearly indistinguishable although a very small change is found below $A < 100$ and near the valley around $A = 180$. The atomic number and neutron number of each fission fragment is determined by the assumption that the proton to neutron number ratio is the same as that of the parent nucleus after correcting for prompt neutron emission, i.e. $Z_p/N_p = Z/(N + N_{loss}/2)$.

We have run calculations in which Gaussian width parameter σ is varied from 4 to 14 and compared with the result with $\sigma = 7$. We then found that the rare-earth peak changes by only +20%,-25% so that the abundance decreases slightly for larger σ . Although the abundances below $A < 100$ and near the valley around $A = 180$ increases as σ increases, these changes do not change the overall distribution drastically, and the conclusions of this article are not affected by fixing $\sigma = 7$.

The quantity α in Eqs. (2) and (3) is the average mass-asymmetry parameter corresponding to the valley of the potential energy surface of the parent nucleus near the scission point for nuclear fission. This has been calculated in the liquid drop model [37] with shell energy corrections determined [38, 39] from the two-center shell model in the three-dimensional shape parameter space comprised of α , the distance between the centers of the two-harmonic oscillators z , and the deformation parameter of the fission fragments, δ . The quantity ω_s is determined as $\omega_s = -0.2(V_s - V_a - 2.0)$ for $V_s - V_a < 2.0$ MeV, and $\omega_s = 0$ otherwise, where V_s and V_a denote the potential values at symmetric and asymmetric valleys, respectively, at the fragment distance z corresponding to scission. This approximate formula is derived to account for the observed rapid change between asymmetric- and symmetric-mass distributions around ^{256}Fm , i.e. V_s is adjusted relative to V_a to reproduce the observed mass distributions of the Fm isotopes with Eq. (1).

For illustration in the present study we have carried out r -process simulations in the fission recycling environment from the NSM outflow models of [14, 16, 17]. As an illustration of the main r -process we take abundances in the ejecta from the MHDJ model of [28]. For the weak r -process we use yields from the NDW models of [6]. The NSM outflow model adopted for the present study is the 3D Newtonian smoothed-particle hydrodynamics (SPH) simulation of [14, 16, 17]. It gives qualitatively similar results to the fission recycling r -process yields calculated in 3D general relativistic SPH simulations [15, 40] and the full 3D general relativistic simulations of [23] in the heavier mass region. The details are different for lighter masses because of the broader range of neutron densities and electron fractions in the particle trajectories in those models.

We emphasize that the models run here can be considered as generic fission recycling models. For specific NSM models we utilize the trajectories from the binary neutron star merger of two neutron stars with $M = 1.0 M_\odot$ each. Although $1.0 M_\odot$ is not the typical neutron star mass [41], it has been shown [14] that the resulting abundances are nearly independent of the neutron star masses in the binary. The hydrodynamic simulations are based upon the SPH method of [42], the equation of state (EoS) of [43, 44], an opacity-dependent multi-flavor neutrino leakage scheme [45], and Newtonian gravity. We use 30 available trajectories [46] of neutron star merger ejecta to calculate the nucleosynthesis. The ejected mass from this binary merger is $\sim 0.01 M_\odot$ [14]. After the end of the hydrodynamics simulation at $t_{\text{fin}} (\sim 15 \text{ ms})$ the thermodynamic evolution can be continued [47] as a free adiabatic expansion.

The reason for the use of these trajectories is that they are publically available [46] and lead to robust fission recycling. Moreover, a main point of this paper is the importance of a fraction of r -process material that involves fission recycling. If some fraction of the ejects in the NSM calculations as in Refs. [13–15, 23, 24] do not involve fission recycling, then this paper deals with the fraction of material in their models that leads to fission recycling, while the other trajectories would be absorbed into what we label as other components.

In contrast to CCSNe, baryons participating in the r -process constitute a large fraction of the total mass-energy in the NSM ejecta. Thus, the nuclear energy released by the r -process nuclear reactions must be included after t_{fin} by an entropy source term,

$$dS = -\epsilon_{\text{th}} \sum_i (m_i c^2 / k_B T + \mu_i / k_B T) dY_i , \quad (5)$$

where a heating efficiency parameter $\epsilon_{\text{th}} \approx 1$ is introduced [14] to account for neutrino energy losses.

The nucleosynthesis calculations were started at a temperature $T = 9.0 \times 10^9 \text{ K}$. At this point all nuclei are in nuclear statistical equilibrium, and the composition is completely determined from the density and charge-per-baryon Y_e of the material ejected from the neutron stars.

At this point the material almost entirely consists of free neutrons plus some heavy seed nuclei with $A \approx 70$.

As the temperature and density decrease, however, the material is evolved using an updated version of the nuclear network code of [48]. The neutron radiative capture rates are as summarized in [48], however, for both the weak and main hot r -process considered here, the abundance patterns mainly depend on the nuclear masses and beta-decay rates but not on the radiative neutron-capture rates. This is because the system proceeds in (n, γ) equilibrium until a rapid freezeout of the neutron abundance. On the other hand, the fission-recycling NSM r -process considered here depends on the radiative neutron-capture rates because, when the temperature is low, the (n, γ) and beta-decay rates (in the so-called "cold r -process") determine the final abundances. In the fission recycling model adopted here, the r -process path terminates in a region where beta-induced fission is much faster than the neutron-induced fission so that the r -process is always terminated by beta-induced fission. We note, however, that this depends upon the treatment of fission barriers and a different treatment (e.g. Ref. [14]) can result in a different mode of fission termination.

Once the r -process path fissions, we utilize the fission fragment distributions given in [36] and also the nuclear masses from the KTUY model [49]. The fission barriers are extracted from the same KTUY model. However, since the KTUY model treats only the symmetric fission, we adopted here the two-center shell model to allow more general fission fragment distributions. The KTUY model has been shown within the GT2 theory to reproduce recent measurements of beta-decay half-lives of exotic neutron-rich isotopes [29]. In a separate forthcoming paper we will summarize a detailed comparison of the predictions of this model with known FFDs.

We also note that there have been numerous studies (e.g. [3, 26]) of the sensitivity of this type of paradigm on various nuclear physics parameters. However, almost all MHDJ (or NDW) models (without shell quenching) show the abundance deficiencies on either side of the closed r -process abundance peaks. Moreover, the NDW and MHDJ supernova models often involve little or no fission recycling. As such, they do not depend on the details of fission rates and fragment distributions.

We note, however, that our NSM calculation (as shown below in Fig. 2) produces a different abundance pattern than that of previous NSM studies [13–15], especially in the region spanning between the 2nd and 3rd r -process peaks. There are two reasons for this difference: 1) The fission fragment distributions (FFDs); and 2) the number of fissioning nuclei contributing to fission recycling and the freezeout of the r -process distribution.

Regarding the FFDs, it has often been noted (e.g. [13–15]) that the elemental abundances from NSM calculations depend strongly on the FFD model. Admittedly this is a major uncertainty in all calculations of fission recycling in the r -process. As noted above, our FFD model is based upon the KTUY model plus a two-center shell

model to predict both symmetric and asymmetric FFDs with up to three components. As such, fissile nuclei in our approach can span a wide mass range ($A=100-180$) of fission fragments. This is illustrated in the upper panel of Fig. 2 that shows the final abundance distribution compared with the FFDs of three illustrative nuclei.

On the other hand, the models of [14] are mostly based upon a simple two fragment distribution as in [50] (or alternatively the prescription of [51]). The assumption of only two fission daughter nuclei tends to place a large yield near the second r -process peak leading to a distribution that looks rather more like the solar r -process abundances. In contrast, the FFDs of [15] are based upon a rather sophisticated SPY revision [52] of the Wilkinson fission model [53]. The main ingredient of this model is that the individual potential of each fission fragment is obtained as a function of its axial deformation from tabulated values. Then a Fermi gas state density is used to determine the main fission distribution. This leads to a multiple hump FFD similar to that considered here, but even with up to four humps. Although this arguably represents a more fundamental approach than that employed in the present work, we prefer the phenomenological FFD approach here as an alternative means to estimate fission yields far from stability.

An even more important difference between the present work and that of previous studies is the termination of the r -process path and the number of fissioning nuclei that contribute to fission recycling and the freezeout of the r -process abundances. The r -process path in our NSM calculations proceeds rather below the fissile region until nuclei with $A \sim 320$, whereas the r -process path in [15] terminates at $A \approx 278$ (or for a maximum $\langle Z \rangle$ for [14]). Moreover, we find that only $\sim 10\%$ of the final yield comes from the termination or the r -process path at $N = 212$ and $Z = 111$, while almost 90% of the $A = 160$ bump shown in Fig. 2 comes from the fission of more than 200 different parent nuclei mostly via beta-delayed fission. This is in contrast to the yields of [15] that are almost entirely due to a few $A \approx 278$ fissioning nuclei with a characteristic four hump FFD. This is the reason why they obtain a solar-like r -process like distribution.

To illustrate this point, in the lower panel of Fig. 2 we compare the yields of our model with a calculation in which we assume that the r -process path is terminated by symmetric fission of nuclei with $A = 285$. Clearly, in this case a solar-like distribution is obtained similar to that of Refs. [13–15]. This clearly highlights the importance of detailed fission probabilities along the r -process path.

Finally, we note that the apparent suppression of the 3rd r -process peak in our final abundances relative to that of other works is caused by the large increase in the rare earth elements resulting from the FFDs of repeated fission recycling.

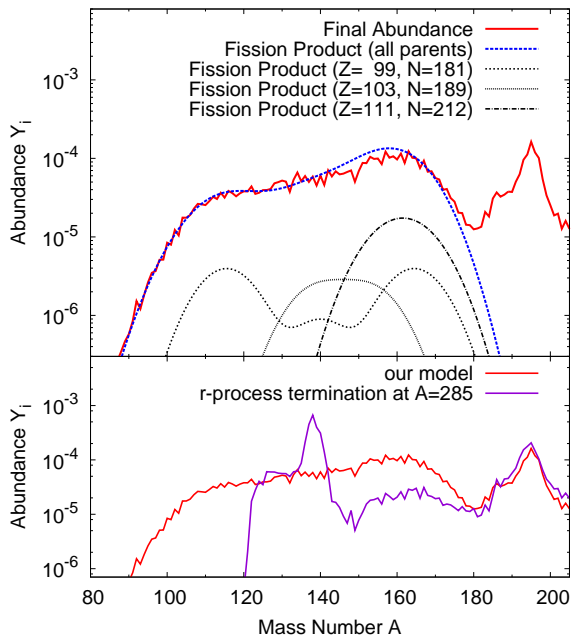


FIG. 2: (Color online) Illustration of the impact of fission yields and fission recycling on the final r -process abundances. Upper panel shows the relative contributions for 3 representative nuclei compared with the final abundance distribution. The lower panel shows the same final r -process yields compared with the distribution that would result if fission recycling were only to occur from parent nuclei at the termination of the r -process path at $A = 285$.

IV. RELATIVE r -PROCESS CONTRIBUTIONS

Figure 2 shows the main result of this paper. The red line on Figure 2 shows the result of our fission recycling nucleosynthesis simulation summed over all trajectories of material ejected from the binary NSM model adopted here. This is compared with the abundances in the ejecta from the main r -process (blue line) from the MHDJ model of [28], and also the NDW weak r -process abundances (green line) produced in the NDW from the $1.8 M_{\odot}$ supernova core model of [6].

The key point of this figure is the important role that each process plays in producing the total abundance pattern of solar-system r -process abundances (black dots with error bars [54]). The total abundance curve from all processes is shown as the black line on Figure 2. The weighting factor $f_{Fission}$ was determined from a normalization to isotopes near $A=145-155$ for the fission recycling (NSM) model. The factor f_{Weak} was determined from a fit to light isotopes near $A=100$ for the NDW model. The MHDJ yields were normalized to the second r -process peak. The best fit (black) line in Figure 2 is for $f_{Fission} = 0.16$ and $f_{Weak} = 4.3$. These relative contributions are consistent with estimated Galactic event rates as described below.

Of particular relevance to the present study is that

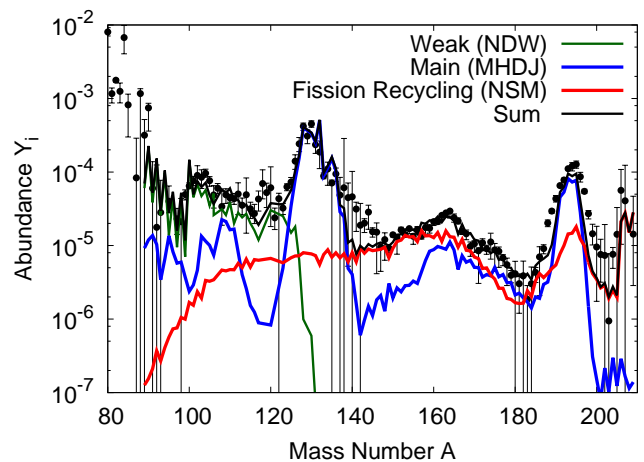


FIG. 3: (Color online) Average final abundance patterns for the fission recycling environment of NSM (red line), the main r -process abundances from the MHDJ model (blue line) and weak r -process (green line) from the NDW. These are compared with the observed [54] r -process abundances in the solar system (black dots). The thin black line shows the sum of all contributions.

the one order of magnitude underproduction of nuclides above and below the $A = 130$ r -process peak shown by the blue line is nearly accounted for by the fission recycling (NSM) and weak r -process (NDW) models. The final r -process isotopic abundances from our NSM model exhibit a very flat pattern due to several episodes of fission cycling. Thus, we find that the fission recycling can resolve most of the underproduction problems for the elements just below and above the abundance peaks in models of the main r -process. The remaining underproduction below the $A = 130$ peak is most likely due to the weak r -process as illustrated on Figure 2.

The main point of this paper is that one can deduce the relative contributions of each r -process model based upon their relative shortcomings. However, it is important to ask whether the inferred fractions, of $\sim 79\%$ NDW, $\sim 18\%$ MHDJ, and $\sim 3\%$ NSM are plausible.

Although there are many uncertainties in the astrophysical and galactic chemical evolution parameters, it is worthwhile to estimate weight parameters $f_{Fission}$ and f_{Weak} from observed Galactic event rates and expected yields. In particular we write

$$f_{Fission} \approx \frac{R_{NSM} M_{r,NSM}}{\epsilon_{MHDJ} R_{CCSN} M_{r,MHDJ}}, \quad (6)$$

and

$$f_{Weak} \approx \frac{R_{CCSN} M_{r,Weak}}{\epsilon_{MHDJ} R_{CCSN} M_{r,MHDJ}}, \quad (7)$$

where $M_{r,NSM}$, $M_{r,MHDJ}$, and $M_{r,Weak}$ are the ejected masses of r -elements from the NSM, MHDJ, and NDW weak r -process models, respectively, while R_{CCSN} and R_{NSM} are the corresponding Galactic event rates of CC-SNe and NSMs. The ejected mass of r -process elements

in the models of [6] is $\approx 2 \times 10^{-5} M_{\odot}$ and nearly independent of assumed core mass. The quantity ϵ_{MHDJ} is the fraction of CCSNe that result in magneto-rotationally driven jets. This was estimated in [10] to be $\sim 1\%$ of the core-collapse supernova rate based upon the models of [55]. However this is probably uncertain by at least a factor of two. Indeed, the fraction could be larger as most massive stars are fast rotators and the conservation of magnetic flux should often lead to high magnetic fields in the newly formed proto-neutron star. Hence, we take this fraction to be $3 \pm 2\%$. The mass of synthesized r -process elements from MHDJs is estimated to be $6 \times 10^{-3} M_{\odot}$ [10] while that of a typical binary NSM is expected to be $2 \pm 1 \times 10^{-2} M_{\odot}$ [14]. If the Galactic neutron star merger rate is $80^{+200}_{-70} \text{ Myr}^{-1}$ [56], and the Galactic supernova rate is, $1.9 \pm 1.1 \times 10^4 \text{ Myr}^{-1}$ [57], then one should expect $f_{Fission} \sim 0.6 \pm 0.4$ and $f_{Weak} \approx 8 \pm 6$ consistent with our fit parameters, and suggesting that this fit may be a way of constraining the relative contribution of NSMs and MHDJs to solar-system material.

We note, however, that other NSM calculations predict about 10^{-4} to $10^{-2} M_{\odot}$ of r -process material to be ejected (e.g. [40, 58]). Adopting a value of $10^{-3} M_{\odot}$ could lead to $f_{Fission} \sim 0.02$, i.e. about an order of magnitude too low. Of course, this needs to be better quantified in more detailed chemical evolution and r -process hydrodynamic models. Nevertheless, based upon the models adopted here, the inferred division of r -process contributions remains at least plausible.

V. UNIVERSALITY OF r -PROCESS ELEMENTAL ABUNDANCES

In the above we have not discussed a very important clue to the origin of r -process abundances. It is by now well established [18] that the elemental abundances in many metal-poor stars show an abundance pattern that is very similar to that of the solar-system r -process distribution, particularly in the range of $55 < Z < 70$. This however, can pose a difficulty [59, 60] for NSM models (either in the present work or in other studies). That is because metal-poor stars are thought to have arrived very early in the history of the Galaxy, whereas NSMs require a relatively long gravitational radiation orbit decay time prior to merger (~ 0.1 Gyr). Whatever the situation, it is of value to examine the impact of the possible late arrival of fission recycling material on the r -process elemental abundance distribution in metal-poor stars.

Figure 4 shows the elemental abundance distribution calculated in two scenarios, i.e. with and without the fission recycling yields of NSMs. These are compared with the observed elemental r -process abundances in two well-studied metal-poor r -process enhanced stars, HD1601617 [61] and CS22892-052 [62]. Here, we note that there is little distinction between the two curves (although the fit is slightly better when the fission recycling yields are included). The reason for this is that the fission recycling

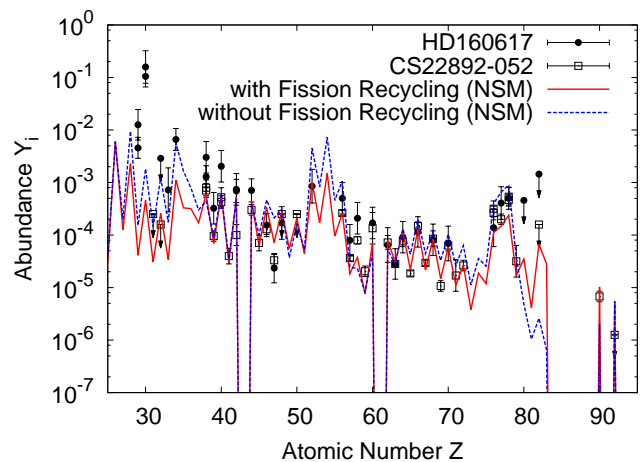


FIG. 4: (Color online) Average final elemental abundances for the total sum from Fig. 2 (solid line) and the contribution without NSMs (dashed line). These are compared with the observed elemental r -process abundances in two well-studied metal-poor r -process enhanced stars, HD1601617 (filled circles [61]) and CS22892-052 (open squares [62]). The curves are arbitrarily normalized at europium ($Z=63$).

environment only contributes about 3% to the total r -process abundance. Although this yield is important to fill in the isotopic abundances above and below the r -process peaks, and also to make the rare-earth bump near $A=160$, there is little apparent difference in the elemental abundances with or without neutron star mergers. Among other things, this is because the region below the peak ($Z \sim 50$) is poorly sampled, and moreover, summing over isotopes to produce elemental averages somewhat washes out the underproduction above and below the r -process mass peaks. Hence, the elemental r -process abundances in metal poor stars do not clearly require that fission recycling occurred early in the Galaxy.

We do note, however that the dispersion in the stars themselves for the lightest elements ($30 < Z < 50$) is consistent with the notion that not all CCSNe contribute both a weak and main r -process. This is consistent with the expectation that the NDW could occur in all CCSNe while the main r -process from the MHDJ will only occur in a limited fraction of CCSNe, i.e. those with rotation and strong magnetic fields.

VI. DISCUSSION

The fits to the abundance distribution (e.g. Figure 2) are as good as or better than most models in the literature. Nevertheless, it is worthwhile, to address some of the detailed deficiencies in both Figures 2 and 4. For example, although the r -process peaks at $A=130$ and 195 along with the rare-earth peak region $A = 145-180$ in Figure 2 are remarkably well reproduced, there are some differences just above the main r -process peaks in the

regions of $A=140-145$ and $200-205$. We note, however, that these isotopes have the largest uncertainties in the r -process abundances themselves as is visible on Figure 2. Hence, these discrepancies may simply reflect the abundance uncertainties, although the possibility remains of a shortcoming in the models for these isotopes.

Similarly, in Figure 4 there is an underproduction of elements at $Z=58$ and 60 . The abundance of Ce ($Z=58$) in Figure 3 is well determined observationally for CS22892-052 as follows: $\log \epsilon(\text{Ce}) = -0.50 \pm 0.07$ [62] and $= -0.38 \pm 0.08$ [63]. This corresponds to the deficient isotopes with $A=140$ and 142 in Figure 2. However, the odd elements with $Z=57$ (La) and $Z=59$ (Pr) are reproduced. This suggests that the odd-even effect in the region of lanthanide elements may be underestimated in the mass model employed here. Nevertheless, the main point of this paper is not to give a precise reproduction of r -process elemental abundances but rather to demonstrate the possibility that fission recycling supplements the underproduced elements. Clearly, a better understanding of the nuclear uncertainties within this context is still needed.

We also note that there is a possible deficiency of Pb ($Z=82$) in Figure 4. This, however, may relate to observational uncertainties. There are two measured Pb abundances for CS22892-052 in [62]. One was a ground-based measurement, while the other was obtained with *HST*. However, both of these values should be considered upper limits. In [62] it was noted that the suggested detections of the two Pb I lines in the ground-based spectra should be nearly 10 times weaker than the $\lambda = 2833.05$ line, that could not be detected in the HST spectrum. Hence, the derived Pb abundance upper limit from the $\lambda = 2833$ line is probably more reliable than the abundances determined from the questionable detections of the other two Pb I lines. Thus, one should abandon the Pb abundance of $\log \epsilon(\text{Pb}) = 0.05$ from the ground-based observation in favor of $\log \epsilon(\text{Pb}) < -0.2$ from the HST observation. We also note that the more recent observation of Ref. [64] also obtains $\log \epsilon(\text{Pb}) < -0.15$. These upper limits are consistent with our calculation.

Another issue worthy of discussion is that of Th ($Z=90$) and U ($Z=92$) production in Figure 4. Th has been observed in a number of metal-poor stars and U in a few. This indicates that the r -process mechanism at work in the early Galaxy could produce the actinide elements and beyond. Although one tends to think that the production of actinide elements requires a fission-recycling r -

process, in fact the production of Th and U is possible even in models that do not lead to fission recycling. For example, the MHDJ models with strong magnetic fields in [65] could produce Th and U in as much as their solar abundances. On the other hand, MHDJ models with weak magnetic fields tend to produce actinides below solar abundances. Hence, the observation of Th and U in metal-poor stars constrains the early astrophysical environment, but does not necessarily require that a fission-recycling r -process (such as the NSM model) contributed to metal-poor stars.

VII. CONCLUSIONS

In summary, we have considered the relative contributions of three generic r -process environments to the solar-system r -process abundances and the abundances in r -process enhanced metal-poor stars. These environments are discussed in the context of neutron star mergers, neutrino driven winds and magnetohydrodynamically driven jets, although these environments should be considered as illustrative and not definitive of the specific r -process environments. Nevertheless, we find that the relative contributions from each environment has the possibility of explaining a unique feature of the r -process abundances and that the relative contributions are plausibly consistent with galactic chemical evolution considerations. Clearly, more work along this line is required to explain details. Nevertheless, we suggest that the possibility that all three general environments occur in detectable amounts in the r -process distribution should be taken seriously in future investigations of the origin of r -process elements.

We thank M. Famiano, K. Nakamura, and J. Hidaka for useful discussions, and also N. Nishimura for MHDJ trajectories from Ref. [28], and S. Rosswog for providing NSM trajectories. We also thank T. Tachibana and H. Koura for providing nuclear reaction data. Numerical simulations were carried out at the Center for Computational Astrophysics, National Astronomical Observatory of Japan. Work at NAOJ was supported in part by Grants-in-Aid for Scientific Research of JSPS (26105517, 24340060). Work at the University of Notre Dame is supported by the U.S. Department of Energy under Nuclear Theory Grant DE-FG02-95-ER40934.

-
- [1] E. M. Burbidge *et al.*, *Rev. Mod. Phys.*, **29**, 547 (1957).
 - [2] B. S. Meyer and J. S. Brown, *Astrophys. J. Suppl. Ser.*, **112**, 199 (1997).
 - [3] K. Otsuki, G. J. Mathews, and T. Kajino, *New Astronomy*, **8**, 767 (2003).
 - [4] G. J. Wasserburg, M. Busso, and R. Gallino, *Astrophys. J.*, **466**, L109 (1996).
 - [5] S. E. Woosley, J. R. Wilson, G. J. Mathews, R. D. Hoffman and B. S. Meyer, *Astrophys. J.* **433**, 229 (1994).
 - [6] S. Wanajo, *Astrophys. J. Lett.*, **770**, L22 (2013).
 - [7] S. Nishimura, *et al.*, *Astrophys. J.*, **642**, 410 (2006).
 - [8] S. Fujimoto, *et al.*, *Astrophys. J.*, **656**, 382 (2007).
 - [9] S. Fujimoto, *et al.*, *Astrophys. J.*, **680**, 1350 (2008).
 - [10] C. Winteler, R. Käppeli, A. Perego, *et al.* *Astrophys. J.*

- Lett., **750**, L22 (2012).
- [11] M. Ono, et al., Prog. Theor. Phys., **128**, 741 (2012).
- [12] K. Nakamura, T. Kajino, G. J. Mathews, S. Susumu, S. Harikae, Int. J. Mod. Phys. **E22**, 1330022 (2014).
- [13] S. Goriely, A. Bauswein and H.-T. Janka Astrophys. J. Lett. 738, L32 (2011).
- [14] O. Korobkin, S. Rosswog, A. Arcones and C. Winteler, Month. Not. Roy. Astro. Soc. 426, 1940 (2012).
- [15] S. Goriely, et al., Phys. Rev. Lett., 111, 242502 (2013).
- [16] T. Piran, E. Nakar and S. Rosswog, Month. Not. Roy. Astro. Soc. 430, 2121 (2013).
- [17] S. Rosswog, T. Piran and E. Nakar, Month. Not. Roy. Astro. Soc. 430, 2585 (2013).
- [18] C. Sneden, J. J. Cowan, and R. Gallino, Ann. Rev. Astron. Astrophys., **46**, 241 (2008).
- [19] M. Arnould, S. Goriely, and K. Takahashi, Phys. Rep., **450**, 97 (2007).
- [20] F.-K. Thielemann *et al.*, Prog. Part. Nucl. Phys., **66**, 346 (2011).
- [21] T. Fischer, S. C. Whitehouse, A. Mezzacappa, F.-K. Thielemann and M. Liebendörfer, Astron. Astrophys. 517, 80 (2010).
- [22] L. Hüdepohl, B. Müller, H.-T. Janka, A. Marek and G. G. Raffelt, Phys. Rev. Lett. 104, 251101 (2010).
- [23] S. Wanajo, et al., Astrophys. J., Lett., **789**, L39 (2014).
- [24] A. Perego, et al., Mon. Not. Roy. Astr. Soc., **443**, 3134 (2014).
- [25] G. J. Mathews and R. A. Ward, Rep. Prog. Phys., **48** 1371 (1985).
- [26] B. Pfeiffer, et al., Nucl. Phys., **A693**, 282, (2001).
- [27] K. Farouqi, et al. Astrophys. J. , **712**, 1359 (2010).
- [28] N. Nishimura, T. Kajino, G.J. Mathews, S. Nishimura, and T. Suzuki, Phys. Rev., **C85**, 048801 (2012).
- [29] S. Nishimura, et al., Phys. Rev. Lett., **106**, 052502 (2011).
- [30] H. Watanabe et al. Phys. Rev. Lett., **111**, 152501 (2013).
- [31] G. Martínez-Pinedo et al., Prog. Part. Nucl. Phys., **59**,199 (2007).
- [32] J. Erler, K. Langanke, H. P. Loens, G. Martínez-Pinedo, and P.-G. Reinhard, Phys. Rev., **C85**, 025802 (2012).
- [33] S. Chiba, H. Koura, T. Maruyama, et al., in *Origin of Matter and Evolution of Galaxies*, AIP Conf. Proc. **1016**, 162 (2008).
- [34] H. Koura, in *Tours Symposium on Nuclear Physics V*, AIP Conf. Proc. **704**, 60 (2004).
- [35] S. Tatsuda, K. Yamamoto, T. Asano, et al., in *Origin of Matter and Evolution of Galaxies*, AIP Conf. Proc. **1016**, 469 (2008).
- [36] M. Ohta, et al., in *Proc. of Int. Conf. on Nucl. Data for Science and Technology*, Nice, France, (2007).
- [37] W. D. Myers and W. J. Swiatecki, Phys. Rev. , **C60**, 014606(1999).
- [38] A. Iwamoto, S. Yamaji, S. Suekane, K. Harada, Prog. Theor. Phys., **55**, 115 (1976).
- [39] K. Sato, S. Yamaji, K. Harada, S. Yoshida, Z. Phys. **A 290**, 149 (1979).
- [40] Bauswein et al. Astrophys. J., 773, **78**, (2013).
- [41] R. Valentim, E. Rangel and J. E. Horvath, Mon. Not. Roy. Astron. Soc., **414**, 1427 (2011).
- [42] S. Rosswog, New Astron. Rev., **53**, 78 (2009).
- [43] H. Shen, H. Toki, K. Oyamatsu, K. Sumiyoshi, Nucl. Phys. A, **637**, 435 (1998).
- [44] H. Shen, H. Toki, K. Oyamatsu, K. Sumiyoshi, Progress Theor. Phys., **100**, 1013 (1998).
- [45] S. Rosswog S. and M. Liebendörfer, MNRAS, **342**, 673 (2003).
- [46] Trajectories from <http://compact-merger.astro.su.se/>
- [47] S. Rosswog, O. Korobkin, A. Arcones, F.-K. Thielemann, and T. Piran, Mon. Not. Roy. Astronom. Soc, **439**, 744 (2014).
- [48] M. Terasawa, K. Sumiyoshi, T. Kajino, G. J. Mathews and I. Tanihata, Astrophys. J. **562**, 470 (2001).
- [49] H. Koura, T. Tachibana, M. Uno and M. Yamada, Prog. Theor. Phys., **113**, 305 (2005).
- [50] I. V. Panov, C. Freiburghaus, and F.-K. Thielemann, Nucl. Phys. **A688**, 587 (2001).
- [51] T. Kodama and K. Takahashi, Nucl. Phys. **A239**, 428 (1975).
- [52] S. Panebianco et al., Phys. Rev. **C86**, 064601 (2012).
- [53] B. D. Wilkins, E. P. Steinberg, and R. R. Chaseman, Phys. Rev. **C14**, 1832 (1976).
- [54] S. Goriely *et al.*, Astron. & Astrophys., **342**, 881 (1999).
- [55] S. E. Woosley and A. Heger, Astrophys. J., **637**, 914 (2006).
- [56] V. Kalogera et al., Astrophys. J. Lett, **614**, L137 (2004).
- [57] R. Dhiel, et al. Nature, **439**, 45 (2006).
- [58] K. Hotokezaka, et al. Phys. Rev. **D 87**, 024001 (2013).
- [59] G. J. Mathews, G. Bazan, and J. J. Cowan, Astrophys. J. , **391**, 719 (1992).
- [60] D. Argast, et al. Astrophys. J. , **356**, 873 (2000).
- [61] I. U. Roederer and J. Lawler, Astrophys. J., **750**, 76 (2012).
- [62] C. Sneden, et al., Astrophys. J., **591**, 936 (2003).
- [63] S. Honda, et al., Astrophys. J., **607**, 474 (2004).
- [64] I. U. Roederer, et al., Astrophys. J., **698**, 1963 (2009).
- [65] N. Nishimura, T. Takiwaki, and F.-K. Thielemann, arXiv:1501.06567